Recognition of Aircraft Wake Vortex Based on Random Forest

WEIJUN PAN[1], HAORAN YIN[1], YUANFEI LENG[1], AND XIAOLEI ZHANG[1,2]

[1]College of Air Traffic Management, Civil Aviation Flight University of China, Guanghan 618307, China
[2]Department of Radiology, Second Affiliated Hospital of Shantou University Medical College, Shantou 515041, China

Corresponding authors: Haoran Yin (1051909592@qq.com) and Xiaolei Zhang (bmezhang@vip.163.com)

ABSTRACT The analysis of aircraft wake vortex is of great significance for the improvement of airspace utilization. To overcome the shortcomings of traditional manual methods which are unable to produce satisfactory results on the great number of wake vortex data with high accuracy recognition, a fast automatic method is proposed based on Random Forests (RF). The development of our model is outlined as follows: (1) A wake vortex dataset that consisted of various aircraft measured by Wind3D 6000 LiDAR was collected at Chengdu Shuangliu International Airport from Aug. 16, 2018 to Oct. 10, 2018. (2) The optimal parameters were determined by grid search by visualizing the characteristic values of wake vortices, to get the optimal RF model, allowing high efficiency as well as improved accuracy. In terms of evaluation metrics, the experimental results showed that the method can effectively recognize the wake data in different situations, exhibiting good robustness.

INDEX TERMS Aircraft wake vortex, LiDAR, random forests, feature extraction.

I. INTRODUCTION

Wake turbulence is a function of lift generated by aircraft that is invisible and harmful to the following aircraft, especially in the take-off or landing phase of flight [1]. The study of wake vortex can be used to standardize the separation standard of wake turbulence, which ensures flight safety and avoiding of wake encounters. Therefore, in the context of limited airspace capacity, conservative wake turbulence separation is the main factor affecting the increase of airspace capacity.

Computational fluid dynamics (CFD) and flow field measurement are two primary methods to study the behavior of aircraft wake [2]. CFD supports the consistent study of wake vortex behavior under various environmental conditions but cannot exhibit a significant impact on aircraft spacing that improves airport capacity [3]. The high precision and resolution of LiDAR make it capable of supporting the most effective field measurement. In particular, the new wake turbulence separation criteria rely on LiDAR measurements and techniques, which have become effective tools for predicting and characterizing aircraft wake vortices under different environmental parameters at different flight stages [4]–[7].

The associate editor coordinating the review of this manuscript and approving it for publication was Abdullah Iliyasu .

However, the wind field data generated by LiDAR also contains non-wake wind field data, which make direct use impossible. In addition, the high difficulty in the measurement of the relative position of aircraft and LiDAR makes the data set not match the correct flight. Particularly, even if ADS-B or QAR data are used, the large amount of data provided by LiDAR require considerable manual processing. Moreover, due to the influence of sensor scanning and environmental parameters, the traditional artificial recognition method cannot provide satisfactory results for the recognition of high accuracy great number of wake vortex data. Therefore, the development of an efficient technique for automatic annotation of wake vortex data is essential.

Machine learning is an effective method that can be employed to divide LiDAR data into non-wake and wake data, but its performance depends on the visualization of LiDAR data and the configuration of the color map at different speeds. In the process of converting data into images, inappropriate color mapping may lead to poor performance and information loss [8]–[10].

To address these issues, the k-nearest neighbor (KNN) [11] and the support vector machine (SVM) [12] methods were used. A new perspective to further understand LiDAR data classification model based on random forests (RF) is provided
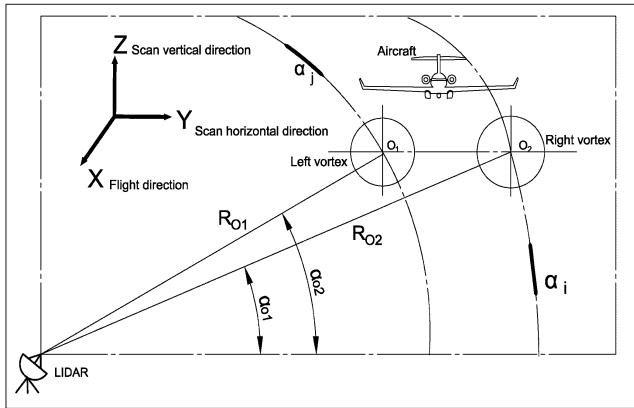
FIGURE 1. The schematic diagram of RHI mode.

in this study [13]. RF is an ensemble supervised machine learning algorithm, which summarizes the output of multiple prediction models to improve the classification accuracy. Briefly, the integration of multiple classifiers yields decrease in variance, especially in the case of unstable classifiers, producing more reliable results [14]. Compared with other machine learning methods, the advantages of RF can be summarized as follows [15]:

· No requirement for dimensionless processing makes RF capable of processing multiple forms of data, which is suitable for the treatment of certain missing attribute values

· The ability of handling high dimensionality data and complexity allows it to overcome data multicollinearity

· It is robust to noise and outliers

· It can directly obtain the each-index contribution to the total risk, avoiding subjective human error assignment.

Since the results of LiDAR products can be supported by information content that extends the gray-scale data, RF is a good prospective tool for wake vortex recognition. In such situations, the proposed model is used in a complementary way. The present data set was collected at Chengdu Shuangliu International Airport (CSIA) from August 16, 2018 to October 10, 2018. The experimental study shows that the robustness to outliers and noise in our RF-based method is useful for the recognition of wake vortices.

The remainder of the paper is organized as follows. The data resources of this work and the proposed methodology are introduced in Section II. Experimental results are presented in Section III and conclusions are drawn in Section IV.

II. MATERIALS AND METHODS
A. DATA SOURCES
The data was obtained by using pulse Doppler LiDAR. The LiDAR detection mode is divided into PPI (plant position indicator) mode and RHI (range height indicator) mode. The data was collected in the laser radar RHI mode, and the schematic diagram of RHI mode is shown in Figure 1. The LiDAR model was wind3D 6000, and the specific parameters are shown in Table 1.

TABLE 1. Specifications of wind3D 6000.

Qualification	Specifications
Wavelength (μm)	1.55
Pulse repetition (kHz)	10
Sampling rate (GHz)	1
Data update rate (Hz)	4
Pulse width (ns)	100-400
Pulse energy (μJ)	150
Measurement range (m)	45-6000
Range resolution (m)	15-50

FIGURE 2. Schematic diagram of the field measurement.

As shown in Figure 2, the position of LiDAR was at point A, and the entrance of runway 02R was at point B. The extension line of the runway center line and RHI mode intersection detection surface was at point C. The distance from LiDAR to point C was 503m, and the distance from entrance to point C was 1,468m. More than 270,000 detection data were collected from August 16, 2018 to October 10, 2018, including A320 series, A330 series, B738 and GLF4.

B. METHODOLOGY
The LiDAR can only measure the velocity at the direction of the line-of-sight (LOS), limited by the principle of the Doppler effect. The LOS velocity, also called radial velocity, is discrete, so the set of the radial velocity of the wind field is defined as V_r:

$$V_r = \{v_r(r_i, \theta_j)\}, \quad i \in [1, n], \, j \in [1, m], \quad (1)$$

where r_i is the i-th range (i.e., the distance from the LiDAR), θ_j is j-th angle (i.e., the pitch angle of the LiDAR), and $v_r(r_i, \theta_j)$ indicates the radial velocity of the point at coordinate (r_i, θ_j); n and m are the number of discrete values of the pitch angle and the number of range gates obtained by LiDAR detection scanning, respectively, and the number of range gates of LiDAR used for field detection was 56.
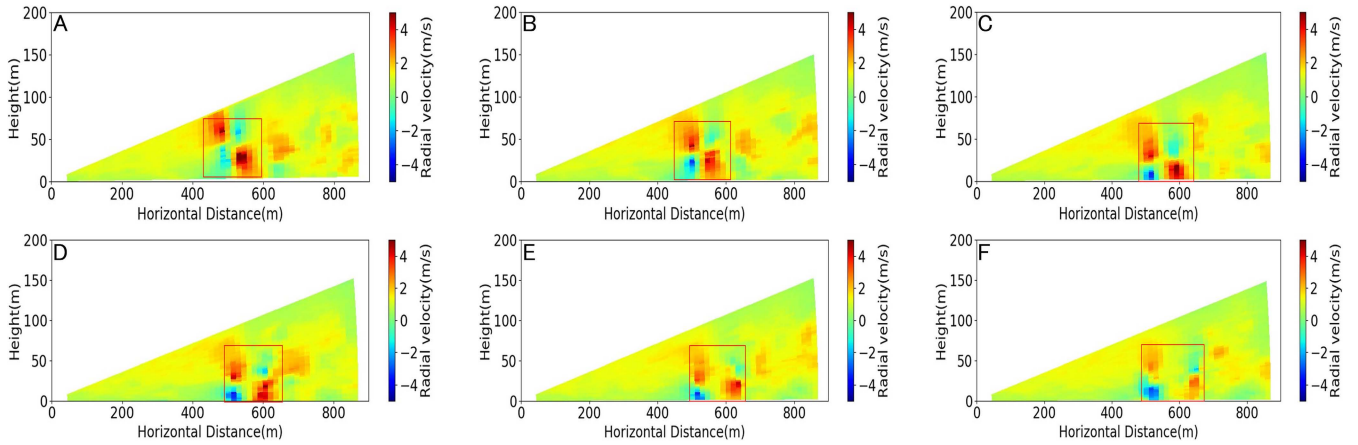
FIGURE 3. Visualization of A320 wake vortex evolution measured by LiDAR.

The azimuth angle is fixed when the LiDAR is in RHI mode. The fast Fourier transform of the pitch angle on the LiDAR received echo was used to obtain the radial wind velocity of the fixed range gate. In detail, the negative value is the velocity close to the LiDAR direction, the positive value is the velocity far from the LiDAR direction. When the LiDAR scans one circle from the set scanning elevation angle, the radial velocity wind field of a section is obtained.

Figure 3 shows part of the wake data under the time evolution detected by LiDAR, where the color bar represents the radial velocity, the wake is shown as a pair of red and green regions, and (A-F) is the time evolution process of the same wake of A320 aircraft.

1) FEATURE EXTRACTION

Three features were used in this paper, namely velocity envelope of different angles or ranges and average background wind field. $D_r(r_i)$, $D_a(\theta_j)$ and $\overline{V_R}$ are introduced as follows:

$$D_r(r_i) = \max(v_r(r_i, \theta_j)) - \min(v_r(r_i, \theta_j)), \quad \forall j \in [1, m],$$
(2)

$$D_a(\theta_j) = \max(v_r(r_i, \theta_j)) - \min(v_r(r_i, \theta_j)), \quad \forall i \in [1, n],$$
(3)

$$\overline{V_R} = \frac{1}{nm} \sum_{i=1}^{n} \sum_{j=1}^{m} v_r(r_i, \theta_j),$$
(4)

where $D_r(r_i)$ and $D_a(\theta_j)$ are the max difference radial velocities at the i-th range r_i and the i-th angle θ_j, respectively. The core position of the vortices can be determined in terms of the difference between the maxima (for the positive envelope) and the minima (for the negative envelope). $\overline{V_R}$ is average background wind field and it is the average value of the radial velocity wind field of a section.

In the construction of the labeled data set with ground-truth wake vortex annotations, the function $D_r(r_i)$ was used to determine the existence of the wake vortex in one
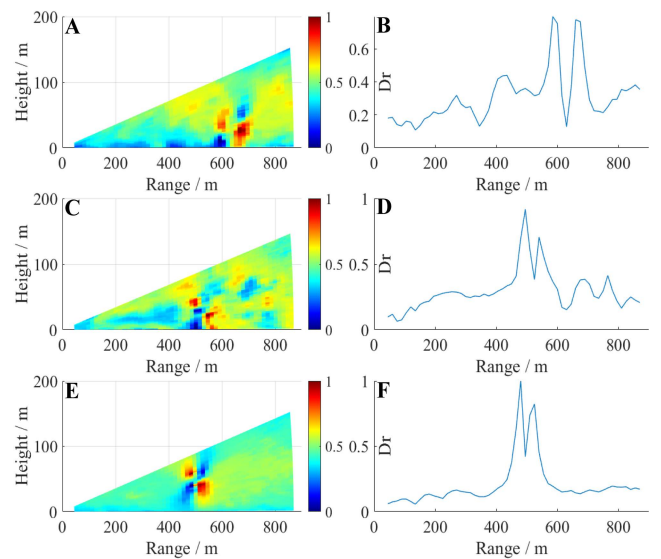

FIGURE 4. Wake vortex location determination. (A), (C), and (E) denote 2D radial velocity distribution of wake vortex for A333, GLF5 and A332, respectively; (B), (D) and (F) are $D_r(r_i)$ of wake vortex for A333, GLF5 and A332, respectively.

scanning measurement, which is similar to Equation 1 of [16]. Figure 4 shows the data with three pronounced bimodal distributions for A333, GLF5 and A332, respectively. The wake vortex range bins where the two peaks appear are determined.

2) RF MODEL

RF is an ensemble learning method for classification that integrates several relatively simple evaluators (i.e., decision trees) to form cumulative effects [17]. Compared with the current algorithms, RF can of assessing the importance of each feature in classification, generate excellent accuracy and run efficiently on large datasets. At present, it has been applied in data mining, big data, bioinformatics, and other fields.

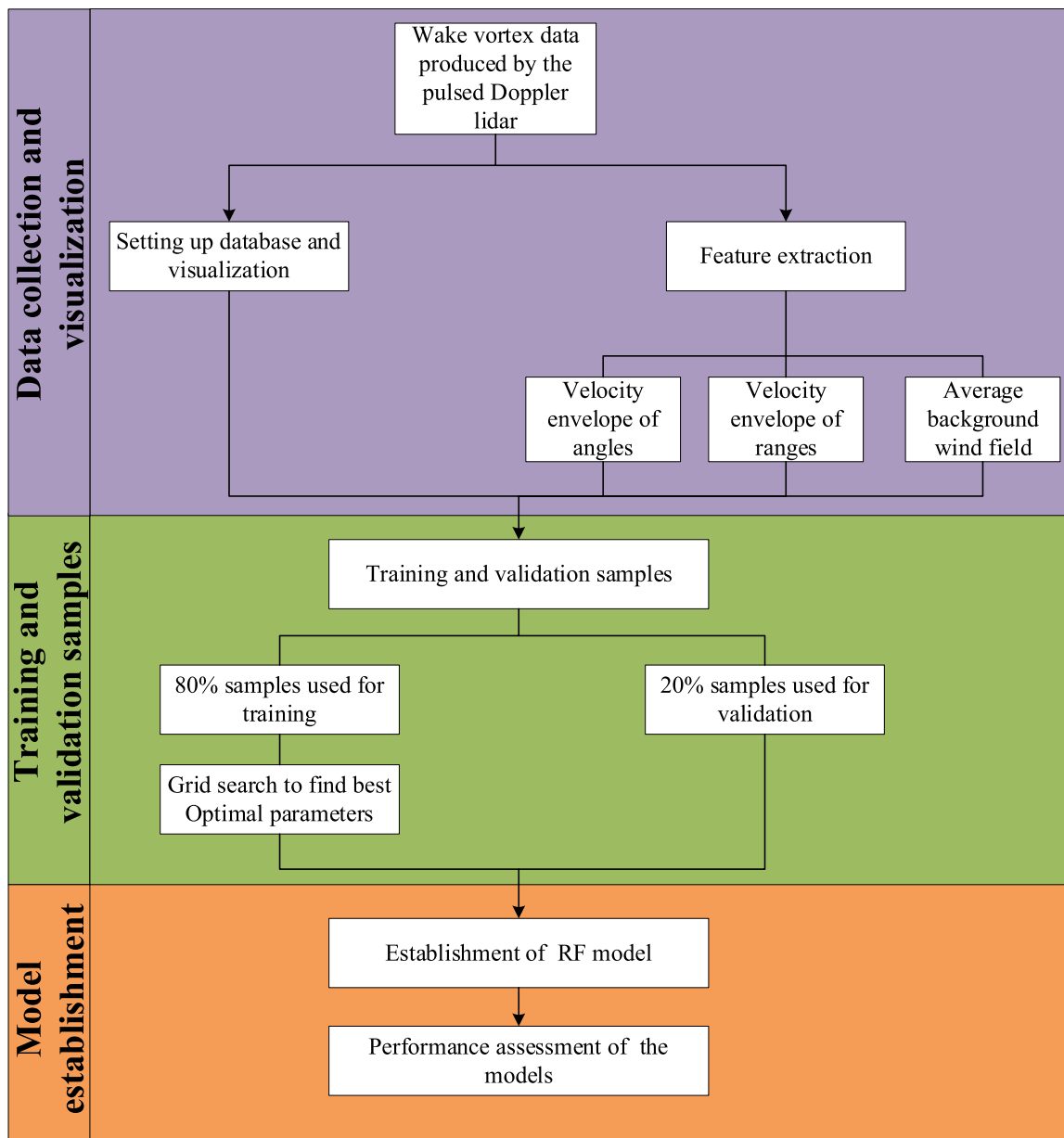The RF algorithm employs the Boostrap sampling method in building decision trees, which repeatedly and

randomly trains N groups with each group being about 2/3 (Bagging) of the original data. In the construction of each tree, m features called the random subspace of M feature variables ($m \leq M$) are randomly selected for the division of internal nodes. Finally, the predicted results of N decision trees are used for voting, to determine the new sample category. A RF model with N decision trees was built in this study, and the test sets scored the performance of the model and ranked the importance of each feature. The calculation method of feature importance score (IS) is summarized as follows:

$$S = \sum (errOOB2 - errOOB1)/N, \qquad (5)$$

For each Decision Tree in the RF, the corresponding out-of-bag data are used to calculate its out-of-bag data error ($errOOB1$). Then random noise interference is added to the features of all samples of out-of-bag data to calculate the error again, which is denoted as $errOOB2$.
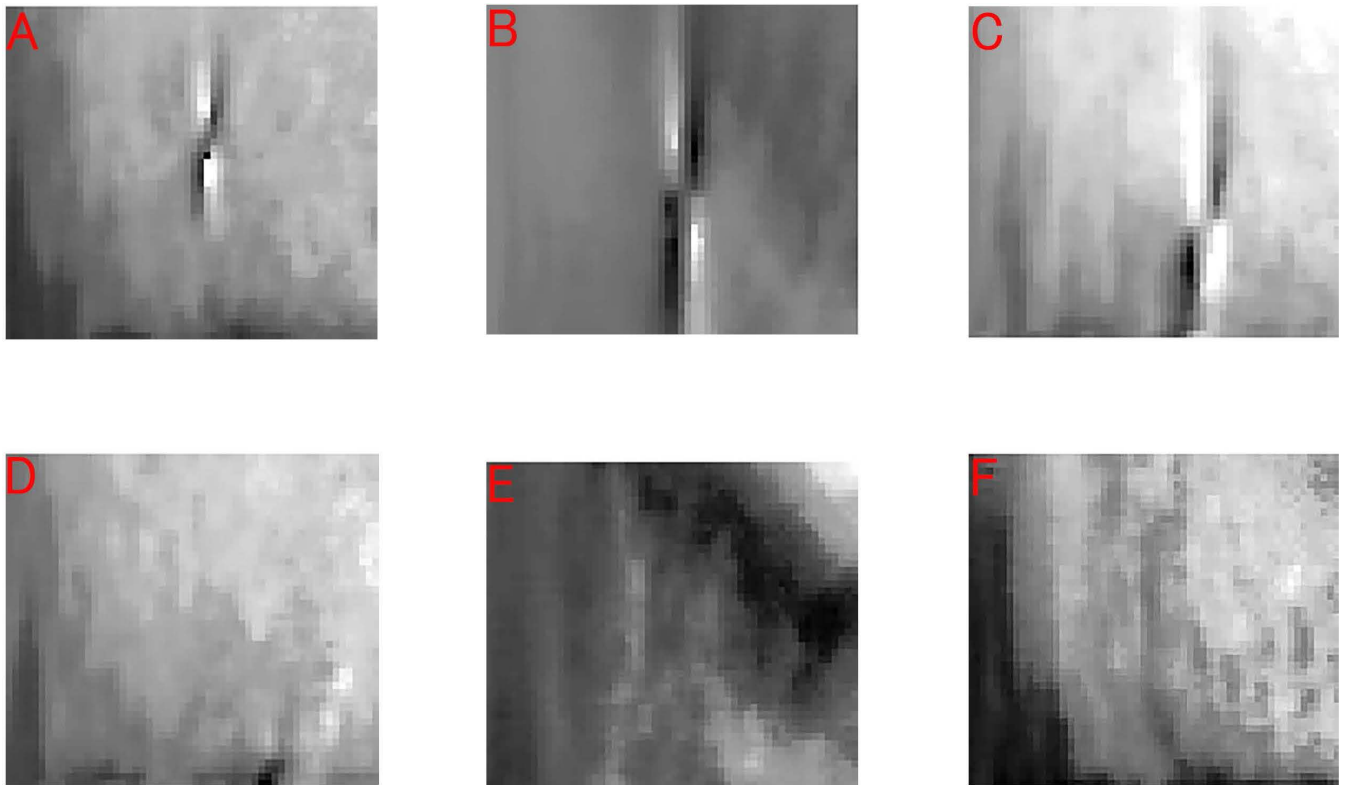
3) WAKE VORTEX RECOGNITION

The flow chart of the aircraft wake vortex recognition algorithm based on RF model is shown in Figure 5, and each part of the algorithm flow is described in detail in Section C.

C. EXPERIMENT

1) EXPERIMENTAL ENVIRONMENT

The experiments were performed on a workstation with 48GB RAM and i7-9700 CPU, using PyCharm 2020.1.1,

FIGURE 6. Visualization of cross-section data in gray scale. For all plots, the x-axis denotes the scan range and the y-axis denotes the scan pitch angle. (A) represents the imaging of weak wake, (B) is the imaging of strong wake, (C) denotes the imaging of strong wake sinking, (D) represents the background wind field behaving relatively uniform, (E) indicates the background wind field behaving relatively strong, and (F) represents the background wind field behaving uneven.

Anaconda 3 and Python 3.8. The scikit-learn package was used for the classification tasks of RF model.

2) DATA PREPROCESSING

The detection models of aircrafts included A320 series, A330 series, B738, GLF4, and others. The LiDAR data of 270,000 samples under good weather was considered, and each sample indicated a given scan pitch angle in degrees. The effective detection data was screened on the pitch angles from 0 to 10 degrees. Therefore, a cross-section in LiDAR data can be visualized as a gray scale image, as shown in the Figure 6, where (A-C) are the images of wakes, and (D-F) indicate the images of non-wakes.

3) MODEL TRAINING

The data set used in the experiment included 2,500 cross-section data, and the eigenvalue data were extracted and labeled. It included 540 data of aircraft wake and 1,960 data of non-wake. According to the labeling ratio, 2,000 data were randomly selected as the training set of the RF model, and the remaining 500 data were selected to be the test set of the model.

To get the optimal parameters of the RF model, the grid search tool GridSearchCV [18] was used to determine the best parameters to achieve the optimal classification performance.

The key terms of GridSearchCV are briefly summarized as follows [19]:

· *Estimator* is used for the implementation of scikit-learn estimator interface when the classifier is to be trained.

· *Parameter grid* denotes parameter keys and a list named as a python dictionary. All the parameter combinations are tested to check the best accuracy.

· *Cross Validation* is used to evaluate learning models by resampling the available data. The purpose of this process is to check the performance of learning models on unseen data, allowing less biased or less optimistic results compared to a simple train-test set split.

The specific simulation parameters are detailed in Table 2, where GridSearchCV was used to optimize RF model parameters.

4) PERFORMANCE ASSESSMENT

In this section, the Accuracy, Recall, Precision, F1_score, receiver operating characteristic (ROC) and area under ROC curve (AUC) [20]–[23] were used as performance metrics to evaluate the classification performance of the RF model when it is applied to the recognition of aircraft wake vortex. The Accuracy is calculated as the ratio between the number of correctly predicted samples to the total number of samples; Recall measures the ratio between the predicted true positive (TP) to the total number of positive predicted samples;

TABLE 2. The specific simulation parameters.

Parameter	Description	Optimum Parameters	Search Range
n_estimators	The number of trees in the forest	90	85~100
max_depth	The deepest depth of the tree	7	1~10
min_samples_leaf	Minimum number of samples on leaf nodes after separation	13	5~20
min_samples_split	Minimum number of samples separated	48	40~60
max_features	The number of randomly selected features per decision tree	"sqrt"	"auto" "sqrt" "log2"

TABLE 3. Test set recognition results.

Method	Accuracy	Recall	Precision	F1_score
RF with default parameters	0.94	0.83	0.89	0.90
RF with optimal parameters	**0.95**	**0.88**	**0.89**	**0.93**
RF with 5-k cross-validation	0.92	0.83	0.85	0.89
KNN	0.77	0.81	0.63	0.79
SVM	0.78	0.83	0.63	0.80

Precision is calculated as the ratio between the predicted TP to the actual total number of positive samples; The F1_score conveys the balance between Precision and Recall; The ROC curves explore the effects on the true positive rate (TPR) and the false positive rate (FPR) as the position of an arbitrary decision threshold is varied, and the AUC with a larger value indicates more accurate recognition. The formulas of Accuracy, Recall, Precision and F1-score are presented in Eqs. (6-8), respectively.

$$Accuracy = \frac{TP + TN}{TP + TN + FP + FN}, \qquad (6)$$

$$Precision = \frac{TP}{TP + FP}, \quad Recall = \frac{TP}{TP + FN}, \qquad (7)$$

$$F1\_score = \frac{2 \cdot Precision \cdot Recall}{Precision + Recall}. \qquad (8)$$

III. RESULTS

In this section, experiments on the wake vortex data set were conducted. To set a general comparison, the experimental results of KNN [11], SVM [12] and RF were considered and the results are summarized in Table 3.

For the default parameters, the classification effect based on the RF model was high, with a recall rate of 0.83, an accuracy rate of 0.89 and an F1-score of 0.90. The results presented by RF with the default parameters were the same as those of 5-k cross-validation and SVM in terms of recall, while the model exceeded the performance of 5-k cross-validation, KNN and SVM in the terms of other evaluation metrics.
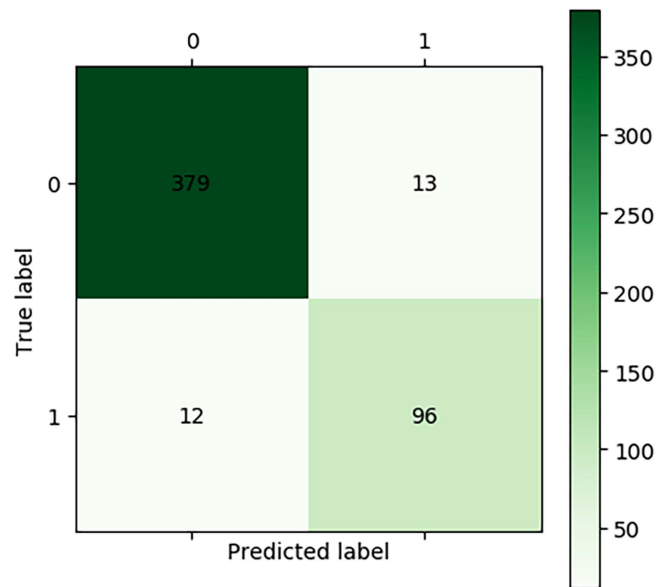
FIGURE 7. Confusion matrix.
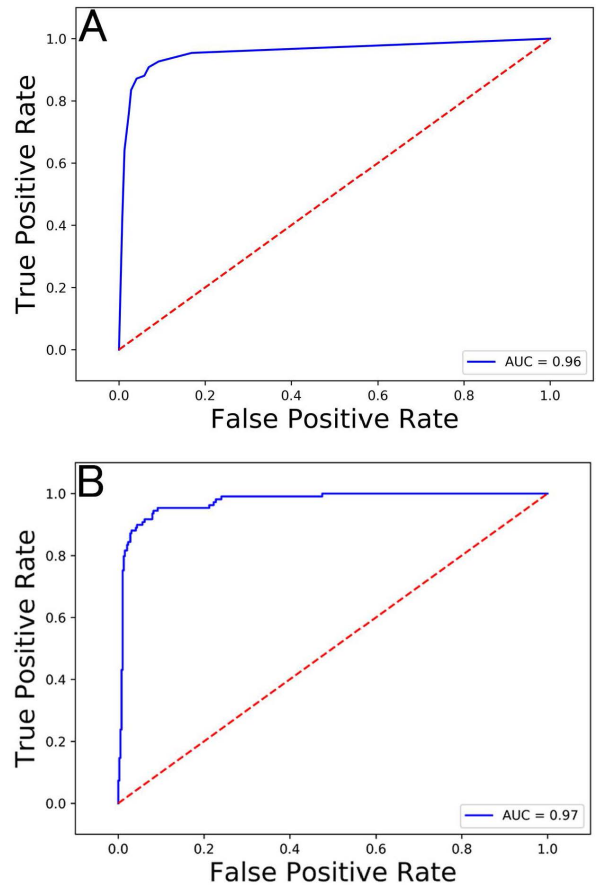
FIGURE 8. (A) The ROC curve of the model under the default parameters; (B) The ROC curve of the model under the optimal parameters.

The RF model with optimal parameters obtained by grid search performed better than its counterpart, giving consistently improved recognition accuracy. Figure 7 shows the confusion matrix of the RF model with the optimal parameters. The test set consisted of 500 data, including

TABLE 4. Prediction results of three aircraft types.

Aircraft type	Number of samples	Number of correctly predicted samples	Prediction accuracy
Light aircraft	15	8	0.533
Medium aircraft	71	67	0.944
Heavy aircraft	22	21	0.955

108 wake data and 392 non-wake data. For the 108 wake data, 96 were predicted correctly, and 379 data of non-wake were predicted correctly among 392 non-wake data.

The ROC curve results are presented to evaluate the generalization performance of the RF model. Figure 8 shows the ROC curve of the RF model under the default parameters and the optimal parameters, respectively. The AUC values of 0.96 and 0.97 show that the RF model under the default parameters and the optimal parameters provides high robustness.

Finally, the experiment on the classification of 108 wake data in aircraft of three types: light aircraft, medium aircraft and heavy aircraft. Table 4 lists the results of the quantitative evaluation.

IV. CONCLUSION

An effective method for processing aircraft wake data and extracting features is proposed in the present paper. The aircraft wake data measured by pulse Doppler LiDAR was collected at Chengdu Shuangliu International Airport from August 16, 2018 to October 10, 2018. A total of 2,500 cross-section data were visualized as gray images, yielding obvious wake vortex characteristics and high recognition degree, by screening the effective detection data on the pitch angles. Experimental results demonstrated that the algorithm based on the random forest classification scheme can effectively recognize aircraft wake data. Using the parameters $n\_estimators = 90$, $max\_depth = 7$, $min\_samples\_leaf = 13$, $min\_samples\_split = 48$ and $max_features = $ 'sqrt', the grid search resulted in the best classification effect: the Accuracy was 0.95, the F1_score was 0.93 and the AUC was 0.97.

REFERENCES

[1] T. Gerz, F. Holzäpfel, and D. Darracq, "Commercial aircraft wake vortices," *Prog. Aerosp. Sci.*, vol. 38, no. 3, pp. 181–208, Apr. 2002.

[2] T. Luan, "Numerical simulation of crosswind effects on aircraft wake-vortex," M.S. thesis College Air Traffic Manage., Civil Aviation Flight Univ. China, Deyang, China, 2019.

[3] J. N. Hallock and F. Holzäpfel, "A review of recent wake vortex research for increasing airport capacity," *Prog. Aerosp. Sci.*, vol. 98, pp. 27–36, Apr. 2018.

[4] F. Köpp, S. Rahm, and I. Smalikho, "Characterization of aircraft wake vortices by 2-μm pulsed Doppler LiDAR," *J. Atmos. Ocean. Technol.*, vol. 21, no. 2, pp. 194–206, Feb. 2004.

[5] M. Harris, R. I. Young, F. Köpp, A. Dolfi, and J.-P. Cariou, "Wake vortex detection and monitoring," *Aerosp. Sci. Technol.*, vol. 6, no. 5, pp. 325–331, Sep. 2002.

[6] F. Holzäpfel, T. Gerz, F. Köpp, E. Stumpf, M. Harris, R. I. Young, and A. Dolfi-Bouteyre, "Strategies for circulation evaluation of aircraft wake vortices measured by LiDAR," *J. Atmos. Ocean. Technol.*, vol. 20, no. 8, pp. 1183–1195, Aug. 2003.

[7] S. Rahm, I. Smalikho, and F. Köpp, "Characterization of aircraft wake vortices by airborne coherent Doppler LiDAR," *J. Aircr.*, vol. 44, no. 3, pp. 799–805, May 2007.

[8] W. Pan, Q. Zhang, Q. Zhang, H. Li, and Z. Wu, "Identification method of aircraft wake vortex based on Doppler LiDAR," *Laser Technol.*, vol. 43, no. 2, pp. 233–237, 2019.

[9] W. Pan, Y. Duan, Q. Zhang, Z. Wu, and H. Liu, "LiDAR aircraft wake vortex recognition based on AlexNet convolutional neural network," *Opto-Electron. Eng.*, vol. 46, no. 7, pp. 121–128, 2019.

[10] W. Pan, Z. Wu, and X. Zhang, "Identification of aircraft wake vortex based on k-nearest neighbor," *Laser Technol.*, vol. 44, no. 4, pp. 471–477, 2020.

[11] Z. Wu, "Study on identification and prediction of aircraft wake vortex using Doppler LiDAR," M.S. thesis, College Air Traffic Management, Civil Aviation Flight Univ. China, Deyang, China, 2020.

[12] W. Pan, Z. Wu, and X. Zhang, "Identification of aircraft wake vortex based on SVM," *Math. Probl. Eng.*, vol. 2020, Oct. 2020, Art. no. 9314164.

[13] W. Zhang, C. Wu, H. Zhong, Y. Li, and L. Wang, "Prediction of undrained shear strength using extreme gradient boosting and random forest based on Bayesian optimization," *Geosci. Frontiers*, vol. 12, no. 1, pp. 469–477, Jan. 2021.

[14] M. Sheykhmousa and M. Mahdianpari, "Support vector machine vs. random forest for remote sensing image classification: A meta-analysis and systematic review," *IEEE J. Sel. Topics Appl. Earth Observ. Remote Sens.*, vol. 13, pp. 6308–6325, 2020.

[15] P. Huang, L. Peng, and H. Pan, "Linking the random forests model and GIS to assess geo-hazards risk: A case study in Shifang County, China," *IEEE Access*, vol. 8, pp. 28033–28042, 2020.

[16] S. Wu, X. Zhai, and B. Liu, "Aircraft wake vortex and turbulence measurement under near-ground effect using coherent Doppler LiDAR," *Opt. Exp.*, vol. 27, no. 2, pp. 1142–1163, 2019.

[17] Y. Meng, M. Yang, S. Liu, Y. Mou, C. Peng, and X. Zhou, "Quantitative assessment of the importance of bio-physical drivers of land cover change based on a random forest method," *Ecol. Inform.*, vol. 61, Oct. 2021, Art. no. 101204.

[18] *sklearn.model_selection.GridSearchCV*. Accessed: 2021. [Online]. Available: https://scikit-learn.org/stable/modules/generated/sklearn.model_selection.GridSearchCV.html

[19] G. S. K. Ranjan, A. Kumar Verma, and S. Radhika, "K-nearest neighbors and grid search CV based real time fault monitoring system for industries," in *Proc. IEEE 5th Int. Conf. for Converg. Technol. (I2CT)*, Bombay, India, Mar. 2019, pp. 1–5.

[20] S. Manimurugan, S. Al-Mutairi, M. M. Aborokbah, N. Chilamkurti, S. Ganesan, and R. Patan, "Effective attack detection in internet of medical things smart environment using a deep belief neural network," *IEEE Access*, vol. 8, pp. 77396–77404, 2020.

[21] S. Latif, Z. Zou, Z. Idrees, and J. Ahmad, "A novel attack detection scheme for the industrial Internet of Things using a lightweight random neural network," *IEEE Access*, vol. 8, pp. 89337–89350, 2020.

[22] R. Soleymani, E. Granger, and G. Fumerag, "F-measure curves: A tool to visualize classifier performance under imbalance," *Pattern. Recognit.*, vol. 100, Article ID 107146, 2020.

[23] X. Zhang, W. Pan, Z. Wu, J. Chen, Y. Mao, and R. Wu, "Robust image segmentation using fuzzy C-Means clustering with spatial information based on total generalized variation," *IEEE Access*, vol. 8, pp. 95681–95697, 2020.

WEIJUN PAN received the Ph.D. degree in computer application technology from Sichuan University, Chengdu, in 2013.

Since 1996, he has been working with the Civil Aviation Flight University of China, Guanghan, China, where he is currently a Professor and the Dean of the College of Air Traffic Management. He has become a leader in the field of air traffic management, air traffic safety, and surveillance. He is the author of more than 50 articles. His research interests include aviation safety, air traffic management, and machine learning.

Dr. Pan acted as an expert or a consultant for various academic organizations such as the Chinese Society of Aeronautics and Astronautics. He hosted more than 30 research projects, such as the National Natural Science Foundation, the CAAC Research Foundation, the Sichuan Province Research Foundation, and international cooperation researches.

HAORAN YIN received the B.S. degree in medical information engineering from the Chengdu University of Traditional Chinese Medicine, Chengdu, in 2019. He is currently pursuing the M.S. degree in transportation with the Civil Aviation Flight University of China.

His research interests include big data, machine learning, artificial intelligence, and aviation safety.

XIAOLEI ZHANG received the Ph.D. degree in control theory and control engineering from Nankai University, Tianjin, China, in 2014.

From 2015 to 2017, he was a Postdoctoral Research Fellow with Shantou University Medical College, Shantou, China. From 2017 to 2021, he was a Lecturer with the College of Air Traffic Management, Civil Aviation Flight University of China, Guanghan, China. He is currently working with the Second Affiliated Hospital of Shantou University Medical College, Shantou, China. He is the author of more than 25 articles. His current research interests include digital signal processing, biomedical engineering, machine learning, and computer vision.

Dr. Zhang was a recipient of the Postdoctoral Support Project of Yangfan Talent Plan from Guangdong Province, in 2016 and 2017.

● ● ●

YUANFEI LENG received the B.S. degree in traffic and transportation engineering from Chang'an University, Xi'an, in 2020. He is currently pursuing the M.S. degree in transportation with the Civil Aviation Flight University of China.

His research interests include artificial intelligence in air traffic management and aircraft wake interval reduction technology.